Gas-Phase Dynamic NMR Study of the Internal Rotation in *N*-Trifluoroacetylpyrrolidine

Cristina Suarez,* Elisabeth J. Nicholas, and Molly R. Bowman

Department of Chemistry, Smith College, Northampton, Massachusetts 01063

Received: December 11, 2002

The barrier to the internal rotation around the C−N bond in *N*-trifluoroacetylpyrrolidine (TFAPYR) was characterized using dynamic NMR spectroscopy. Kinetic parameters, $\Delta G^{\ddagger}_{298} = 71.4(1.2)$ kJ mol^{-1}, $\Delta H^{\ddagger} = 67.9(1.4)$ kJ mol^{-1}, and $\Delta S^{\ddagger} = -11.8(4.0)$ J mol^{-1}), were found to be lower in the gas phase than in solution. The pyrrolidine ring substituent in TFAPYR reduces the bulkiness around the C−N amide bond, stabilizing the ground state and increasing the value of the internal rotation barrier, $\Delta G^{\ddagger}_{298}$, compared to *N,N*-dimethyl- and *N,N*-diethyltrifluoroacetamide. The magnitude of $\Delta G^{\ddagger}_{298}$ in TFAPYR is also comparable to that found in primary amide bonds in peptides, emphasizing the importance of having a relatively small energy difference between cis and trans conformations in proline's role as a switch in protein signaling.

Introduction

In an effort to understand how substitution affects the rotational barrier around the C−N amide bond, variable-temperature dynamic NMR (DNMR) spectroscopy has been used extensively in the study of both solvated[1−3] and gas-phase amides.[4,5] The amide bond is a key feature in peptide dynamics and its restricted rotational behavior is a critical determinant of protein conformation in general.

Substantial effort has been made to study experimentally and theoretically the electronic and steric effects of substitution on the rotational barrier of amides, particularly formamides and acetamides.[1−5] These systems were chosen because they serve as amide templates with substituents akin to the variety of side chains present in the 20 gene-coded amino acids. Proline (Pro), hydroxyproline, and the recently discovered pyrrolysine[6] differ from the other common amino acids in having a secondary amino group, a result of having the amine nitrogen cyclized with the side chain. This creates a unique type of peptide bond (Figure 1).

This type of peptide bond seems to be even more rotationally restricted than the more typical primary amide peptide bond. The five-membered ring not only seems to restrict the conformational freedom available to the peptide but also causes the loss of H bonding capability of the amino nitrogen, giving proline a unique role in the secondary structure of its proteins.[7] The local environment surrounding a residue and the height of the barrier to internal rotation influence the relative size of the populations of cis and trans peptide conformations. Yet, while less than 1% of peptide bonds overall are found to have a cis configuration, approximately 5% of proline residues have the same cis preference.[8] Recent findings by Andreotti et al. have shown that the cis−trans isomerization of certain proline residues may play an important regulatory role as switches of catalytic activity.[9]

In the present study, we are interested in the gas-phase and solution kinetic characterization of the hindered internal rotation around the C−N bond in *N*-trifluoroacetylpyrrolidine (TFAPYR, Figure 2) as a model for a Xaa-Pro peptide. TFAPYR is well-
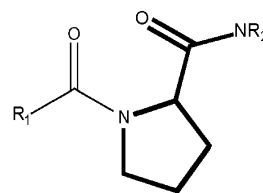

Figure 1. A Xaa-**Pro**-Xaa peptide. The proline residue is in bold and the peptide bond of interest is the one occurring between the first carbonyl and the nitrogen on the pyrrolidine ring.
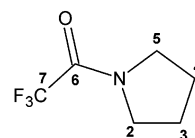

Figure 2. *N*-Trifluoroacetylpyrrolidine (TFAPYR) showing carbon numbering used throughout this work.

suited for this study because its relatively high volatility allows both solution and gas-phase measurements. This study reports the Gibbs free energy ($\Delta G^{\ddagger}_{298}$), activation enthalpy ($\Delta H^{\ddagger}$), and activation entropy ($\Delta S^{\ddagger}$) differences describing the rotational barrier in TFAPYR in the gas phase and in different solutions (toluene-d_8, 1,1,2,2-tetrachloroethane-d_2, and neat). A theoretical ground-state geometry for TFAPYR calculated at the MP2/6-311+G* computational level is also included to understand better the effect of a cyclic substitution on amide geometry. This is the first time a cyclic-substituted amide has been studied in the gas phase.

Experimental Section

Synthesis of TFAPYR. A solution of 0.1 mol (8.4 mL) of pyrrolidine in 10 mL of anhydrous ether was cooled to 273 K in a salt−ice bath, and 10 mL of a solution of anhydrous ether containing 0.05 mol of trifluoroacetic anhydride was added slowly with stirring. After the addition was complete, the reaction mixture was allowed to warm to room temperature and left to equilibrate for 30 min before distilling under reduced pressure. After a small forerun (∼2 mL), a single fraction (6.5 mL) distilling at 350 K (10 Torr) was collected. The distillate contained pyrrolidine, trifluoroacetamide, and the pyrrolidinium

* To whom correspondence should be addressed. Phone: (413) 585-3838. Fax: + 1 (413) 585-3786. E-mail: csuarez@smith.edu.

Internal Rotation in *N*-Trifluoroacetylpyrrolidine

J. Phys. Chem. A, Vol. 107, No. 17, 2003 **3025**

trifluoroacetate salt. Upon cooling, the pyrrolidinium trifluoro-acetate salt crystallized, and the remaining liquid, composed of primarily *N*-trifluoroacetylpyrrolidine, was decanted and passed through a 1×5 cm^2 column of dry alumina to remove the remaining salt. The column eluant (3.5 mL, 54% overall yield) was a clear, colorless liquid. ^{1}H and ^{13}C NMR confirmed the identity of the eluant to be *N*-trifluoroacetylpyrrolidine.

NMR Sample Preparation. Deuterated solvents were obtained from Aldrich. Toluene-d_8 and 1,1,2,2-tetrachloroethane-d_2 were both 99.5+ atom % D; chloroform-d_1 was 99.8 atom % D. All solvents were used without further purification. It is well established that solvent−amide and amide−amide association, as well as other solvent properties, affect reaction rates; therefore, TFAPYR concentrations for NMR solution samples were kept below 15 mol %.[10] Solution samples were prepared by placing either a 5% (^{1}H NMR study) or 10% (^{13}C DNMR study) solution of TFAPYR in the appropriate solvent and a drop of tetramethylsilane (TMS) as a resolution and frequency standard in 5-mm NMR tubes. For samples subjected to high temperatures, a plug was also inserted in the tube to minimize refluxing and evaporation effects within the active volume. Samples were run from low to high temperatures to avoid condensation outside this active volume.

Gas-phase NMR samples were prepared in 3-cm-long restricted volume tubes constructed from Wilmad high-precision glass. The outside diameter of these tubes was 8.89 mm to allow the tubes to fit inside a standard 10-mm Wilmad NMR tube. Neat TFAPYR was degassed through several freeze−thaw−pump cycles before allowing the vapor pressure at ambient temperature to fill the restricted volume tube. Sample-handling techniques and the vacuum system used in the preparation are similar to those described in Ross et al.[11] The gas TFAPYR sample contained 0.7 Torr of TFAPYR, 0.5 Torr of TMS, and 500 Torr of argon as a bath gas. Gas-phase amide internal rotation rate constants do not exhibit pressure dependence at these pressures.[12]

NMR Measurements. ^{1}H NMR measurements for gaseous TFAPYR were performed on a Bruker AMX500 using a 10-mm variable temperature (VT) probe with proton observation at 500.13 MHz. All measurements were made on spinning samples in the unlocked mode. Acquisition times were 1.61 s/scan with a pulse length of 35 μs and a delay time of 1 s. Short delay times are typical of gas-phase NMR because of short relaxation times. Typically, 2000 scans were collected at each temperature and stored in 16 K of memory. A sweep width of $\pm$5102 Hz was used for all spectra, giving a digital resolution of 0.311 Hz/point. The resulting gas-phase spectra had typical signal-to-noise (S/N) ratios of 200:1. A common exponential-line-broadening factor of 1 Hz was applied to all collected spectra after Fourier transform to enhance S/N. Probe temperature calibration was performed using two 36 gauge copper−constantan type "T" thermocouples placed inside a nonspinning dummy gas sample tube. The temperature gradient between the top and bottom of the sample never exceeded 0.4 K. Samples were allowed to equilibrate for 20 min once a stable temperature was achieved. All temperatures used in this study are calibrated temperatures.

^{1}H NMR measurements for the neat and the 5% solutions of TFAPYR were performed on a JEOL Eclipse 400 with a 5-mm VT probe with proton observation at 399.78 MHz. All measurements were made on spinning samples in the locked mode (except the neat sample). Acquisition times varied from 3 to 5 s/scan with pulse angles between 15° and 60° and a common delay time of 4 s. Typically, eight scans were collected at each

temperature and stored in 16K of memory. Digital resolutions better than 0.37 Hz/point were obtained. The resulting solution spectra had typical S/N ratios greater than 1500:1. A common exponential-line-broadening factor of 0.2 Hz was applied to all collected spectra prior to Fourier transform to enhance S/N.

^{13}C NMR measurements for the neat and the 10% solutions of TFAPYR were performed on a Bruker Avance 400 with carbon observation at 75.47 MHz. All measurements were made on spinning samples in the locked mode (except the neat sample). Acquisition times were between 0.54 and 2.16 s/scan with a pulse length of 7.50 μs and a delay time of 2 s. Typically, 1000 scans were collected at each temperature (except for the neat TFAPYR sample for which only 400 scans were necessary) and stored in 16K of memory. Digital resolutions better than 0.92 Hz/point were obtained. The resulting solution spectra had typical S/N ratios greater than 100:1. A common exponential-line-broadening factor of 2 Hz was applied to all collected spectra prior to Fourier transform to enhance S/N.

Calibration of solution temperatures in both spectrometers was performed using a vacuum-sealed 100% ethylene glycol sample. The difference in chemical shifts for the two ethylene glycol peaks was measured between 273 and 423 K and fitted to a published chemical shift difference/sample temperature correlation.[13] Samples were allowed to equilibrate for 20 min once a stable temperature was achieved. All temperatures used in this study are calibrated temperatures and are accurate to $\pm$0.1 K.

Rate Analysis. Rate constants were calculated using the computer program DNMR5.[14] This program uses the complete band shape (CBS) method and an iterative, nonlinear least-squares regression analysis to obtain the best fit to the experimental NMR spectrum. Gas-phase rate constants were extracted from the ^{1}H NMR exchanging spectra using the A$_2$ $\rightleftarrows$ B$_2$ portion (protons attached to C-2 and C-5) of the ring A$_2$C$_2$ $\rightleftarrows$ B$_2$D$_2$ spin system. No $^5J_{HF}$ coupling was observed, probably because of the inherent natural line broadening of gaseous resonances. Solution rate constants were extracted from ^{13}C NMR exchanging spectra using a ACX$_3$ $\rightleftarrows$ BDX$_3$ spin system, where the X$_3$ spins account for observable $^4J_{CF}$ coupling between CF$_3$ and C-2.

The CBS method of analysis first requires the measurement of chemical shifts, coupling constants, and natural transverse relaxation times (T_{2nat}) in the absence of exchange to separate spectral changes due to natural temperature dependence from those due to exchange. The systems were all studied in temperature ranges in which exchange was apparently absent and the parameters' natural temperature dependence could be determined. Coupling constants showed no temperature dependence in any of the systems studied. On the other hand, chemical shifts and T_{2nat} exhibited a dependence on temperature in most situations. Whenever a temperature dependence of either chemical shifts or T_{2nat} was found, a linear relationship was assumed and adjusted parameters were estimated for the exchanging temperatures.

The effective T_2 provided to the DNMR5 program was constructed from the temperature-adjusted T_{2nat}, a magnetic field inhomogeneity contribution estimated from the line width of the reference, TMS, and the exponential-line-broadening factor. Rate constants in the exchange region were obtained by iterating on spectral origin, baseline height, and baseline tilt. All other parameters were adjusted to the appropriate temperature and held constant.

In the calculation of the kinetic activation parameters, the Eyring equation was used to obtain $\Delta H^{\ddagger}$ and $\Delta S^{\ddagger}$. A value of

TABLE 1: Chemical Shifts[a] (ppm) and Coupling Constants (Hz) of Gaseous and Solution TFAPYR[b]

	H$_2$-C-2	H$_2$-C-3[c]	H$_2$-C-4[c]	H$_2$-C-5	C-6	C-8
			Gas			
ν_H	3.619	1.933	1.845	3.530		
$^3J_{HH}$	6.2			6.9		
			Toluene			
ν_H	2.982	1.181	1.112	3.076		
ν_C	46.10	26.09	23.24	47.19	155.00	117.30
$^3J_{HH}$	6.9			6.7		
J_{CF}	3.7	1.5	*d*	*d*	35.4	288.2
			1,1,2,2-Tetrachloroethane			
ν_H	3.609	1.988	1.895	3.530		
ν_C	46.53	26.19	23.43	47.43	155.24	116.31
$^3J_{HH}$	6.9			6.9		
J_{CF}	3.7	1.5	*d*	*d*	36.9	287.5
			Neat			
ν_H	3.637	2.021	1.913	3.495		
ν_C	47.34	26.96	24.15	48.17	155.80	117.80
$^3J_{HH}$	7.0			7.0		
J_{CF}	3.7	1.5	*d*	*d*	36.1	287.5

[a] All chemical shifts are referenced to TMS signals set to 0.000 ppm (gaseous TMS resonates ~3 ppm downfield from solution TMS). [b] Uncertainties in chemical shift values are ca. ±0.001 ppm for ^{1}H and ca. ±0.01 ppm for ^{13}C signals; coupling constants carry uncertainties on the order of ca. ±0.4 Hz for $^3J_{HH}$ and ca. ±0.9 Hz for J_{CF}. [c] $^3J_{HH}$ for C-3 and C-4 were not extracted from the pseudoquintets; the value of ν_H was obtained from the frequency of the strongest line within the multiplet. [d] Not observable.

0.5 was assigned to the transmission coefficient (κ). The Gibbs free energy of activation, $\Delta G^{\ddagger}_{298}$, was obtained from $\Delta G^{\ddagger} = \Delta H^{\ddagger} - (298\ \text{K})\Delta S^{\ddagger}$ assuming $\Delta H^{\ddagger}$ and $\Delta S^{\ddagger}$ to be independent of temperature.

Computational Methods. Ground-state geometries were first optimized at the B3LYP/G3-11+G* level followed by an MP2 calculation with the 6-311+G* basis set using the program Gaussian 98.[15]

Results

Comparison of the gas-phase and solution results indicates considerable medium effects. At room temperature, both gaseous and solution TFAPYR ^{1}H NMR spectra exhibit four distinct sets of signals: two triplets (downfield) and two pseudoquintets (upfield). The triplets correspond to protons attached to carbons C-2 and C-5, and the pseudoquintets are actually multiplets resulting from non-first-order behavior of the protons attached to carbons C-3 and C-4. In all solutions at room temperature, the ^{13}C NMR spectra of TFAPYR exhibit two quartets downfield (C-6 and C-7 quartets due to C−F coupling) and four apparent singlets upfield corresponding to C-5, C-2, C-3, and C-4. Table 1 lists the corresponding ^{1}H and ^{13}C chemical shifts for gaseous and solution TFAPYR.

Assignment of the ^{1}H and ^{13}C NMR signals to the ground-state structure of TFAPYR in the different solvents was made using J_{HF} values, aromatic solvent shifts, and 2D COSY and HETCOR sequences. Coupling between fluorine and hydrogen, J_{HF}, was observed in a degassed sample of TFAPYR in CDCl$_3$. Under these conditions, small quartets due to the spin−spin interaction between fluorines (CF$_3$) and protons (CH$_2$) were observed within each triplet. Observable H−F quartets yield larger $^5J_{HF}$ values for the hydrogens assigned to C-2 (0.89 Hz) than for the hydrogens assigned to C-5 (0.64 Hz) because of the proximity of the C-2 to the CF$_3$ group. This is consistent with previous studies of other trifluoroacetamides.[16,17]
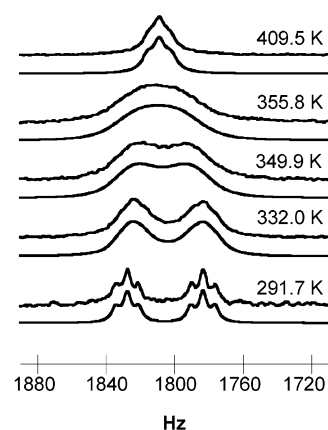

Figure 3. Temperature-dependent gas-phase 500 MHz ^{1}H NMR spectra of TFAPYR protons attached to C-2 and C-5.
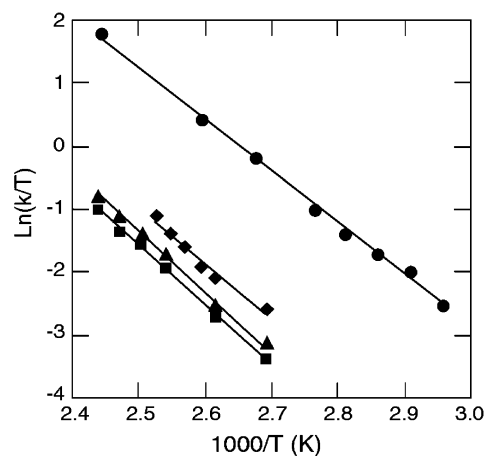

Figure 4. Eyring plots of gas-phase and solution TFAPYR exchange rate constants: (■) 1,1,2,2-tetrachloroethane; (◆) toluene; (▲) neat; (●) gas.

Figure 3 shows temperature-dependent gas-phase ^{1}H NMR spectra of TFAPYR exhibiting exchange broadening of the C-2 and C-5 methylene resonances. Upper traces correspond to experimental spectra, while lower traces correspond to DNMR-simulated line shapes at their respective temperatures. Below 294 K, two separate signals can be observed for C-2 and C-5, while beyond 393 K, only one signal represents the fast exchange between the two distinct magnetic environments.

The Eyring plots, obtained from the rate constants extracted using total-line-shape analysis of all four systems, are presented in Figure 4. Table 2 lists the experimental rate constants (k) characterizing the internal rotation around the C−N bond in gaseous, neat, and 10% (v/v) solution TFAPYR. Table 3 lists the values of the kinetic parameters, $\Delta G^{\ddagger}_{298}$, $\Delta H^{\ddagger}$, and $\Delta S^{\ddagger}$, obtained from those rate constants. Finally, Table 4 summarizes and Figure 5 illustrates the calculated MP2 geometry for the ground state of TFAPYR.

Discussion

In both the gas phase and solution, the ^{1}H NMR spectra of TFAPYR seem to follow traditional amide assignment patterns. Protons trans to the oxygen resonate at higher frequencies than those cis (except in toluene-d_8 in which as in all aromatic solvents the resonance absorption belonging to the protons trans to the carbonyl is shifted farther upfield than the cis proton absorption[1]). Coupling constants, both J_{HH} and J_{HF}, appear to be of the same order and relative magnitude as those observed in other trifluoracetamides.

Internal Rotation in *N*-Trifluoroacetylpyrrolidine

J. Phys. Chem. A, Vol. 107, No. 17, 2003 **3027**

TABLE 2: Exchange Rate Constants (*k*, s⁻¹) for Gas-Phase and Solution TFAPYR

T (K)	gas	neat	toluene 10% (v/v)	1,1,2,2-tetrachloroethane 10% (v/v)
338.0	28.9(1.8)			
344.0	44.7(2.5)			
349.9	63.7(3.7)			
355.9	91.1(5.3)			
361.9	137.6(7.7)			
371.1		16.8(0.9)	27.5(1.4)	12.9(0.6)
373.8	300.6(25.6)			
382.3		32.2(1.6)	47.0(2.4)	25.3(1.3)
385.7	603.8(49.6)		60.4(3.0)	
389.0			79.5(4.0)	
392.4			98.9(5.0)	
393.5		69.9(3.5)		57.2(3.0)
395.7			137.6(7.4)	
399.1		102.8(5.1)		85.4(4.3)
404.7		136.1(6.8)		104.6(5.3)
409.5	2556.5(240.6)			
410.3		191.6(9.6)		155.0(8.0)

TABLE 3: Internal Rotation $\Delta G^{\ddagger}_{298}$, $\Delta H^{\ddagger}$, and $\Delta S^{\ddagger}$ in Gas-Phase and Solution TFAPYR

	gas	toluene 10% (v/v)	1,1,2,2-tetrachloroethane 10% (v/v)	neat
$\Delta G^{\ddagger}_{298}$ (kJ mol⁻¹)	71.4(1.2)	78.6(2.5)	80.9(1.5)	80.4(0.1)
$\Delta H^{\ddagger}$ (kJ mol⁻¹)	67.9(1.4)	75.0(3.2)	77.9(2.0)	78.0(0.1)
$\Delta S^{\ddagger}$ (J mol⁻¹)	−11.8(4.0)	−12.0(8.3)	−10.0(5.0)	−7.8(0.1)

TABLE 4: Computational Molecular Parameters (MP2/6-311+G*) for the Ground-State Geometry of TFAPYR^a

r_{C6N}	1.350	∠OC6N	124.65	τ_{OC6C7F}	109.38
r_{C6O}	1.226	∠C7C6N	115.73	τ_{OC6NC5}	−0.90
r_{NC5}	1.473	∠FC7C6	111.86	τ_{OC6NC2}	−176.06
r_{NC2}	1.475	∠C6NC5	118.33	$\tau_{C2C3C4C5}$	
r_{C7C6}	1.545	∠C6NC2	129.18		
r_{C7F}	1.349	∠C5NC2	112.33		

^{a} Bond lengths are in Å, and angles and dihedral angles are in deg.
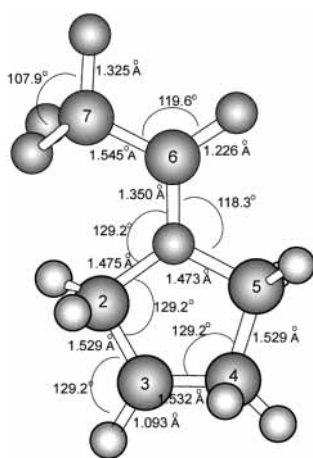
Figure 5. Computed geometry (MP2/6-311+G*) for *N*-trifluoroacetylpyrrolidine.

There are three main conformational processes that dominate the stereodynamics of *N*-acetyl-subtituted pyrrolidines: nitrogen inversion, ring pseudorotation, and internal rotation around the C−N bond. In this TFAPYR study, the internal rotation around the C−N bond was the only process observed.

The nitrogen inversion barrier in TFAPYR is expected to be too small to be observed by DNMR. In trialkylamines, the process of nitrogen inversion changes the geometry of the pyramidal ground state (GS) conformation to a planar transition state (TS). When the nitrogen is part of a strained ring system, the TS is destabilized relative to the GS and a higher nitrogen inversion barrier is expected. Experimental values obtained for *N*-methylaziridine in C₆H₁₂ (79.5 kJ mol⁻¹)[18] and *N*-methylpyrrolidine in Freon solvents (33 kJ mol⁻¹)[19] confirm that less-strained rings systems (pyrrolidine vs aziridine rings) yield lower barriers to nitrogen inversion. Acetylation of the amine further lowers the barrier. The pure p lone pair orbital of the TS has better symmetry for $p_\pi - p_\pi$ overlap than the lone pair in the GS with its mix of s and p hybridization. The barrier to nitrogen inversion of *N*-acetylaziridine in CH₂CHCl has an experimental value of <29 kJ mol⁻¹ [20] compared to the previously cited *N*-methylaziridine (79.5 kJ mol⁻¹), so a large drop in barrier height is expected for *N*-acetylpyrrolidines and in particular TFAPYR in terms of lower ring strain and acetylation.
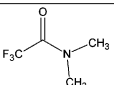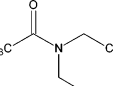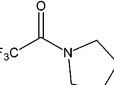
Similarly, barriers to ring pseudorotation in five-membered rings start at an order of magnitude lower (0−17 kJ mol⁻¹) than those to nitrogen inversion.[21] Therefore, ring pseudorotation is expected to be too fast to be observable in this TFAPYR DNMR study.

On the other hand, the barriers for internal rotation around the amide bond are known to fall within DNMR limits (20−85 kJ mol⁻¹).[22] In our study, the splitting patterns observed in the ¹H exchanging NMR signals of TFAPYR (two triplets, hydrogens attached to C-2 and to C-5, and two pseudoquintets, hydrogens attached to C-3 and to C-4) and the number of ¹³C exchanging NMR signals match those expected if fast nitrogen inversion, fast ring pseudorotation, and slow internal rotation all take place. Therefore, the $\Delta G^{\ddagger}_{298}$, $\Delta H^{\ddagger}$, and $\Delta S^{\ddagger}$ values measured for TFAPYR in this gas-phase/solution study can be unambiguously assigned to the internal rotation around the C−N amide bond.

Several magnetic field strengths were used in the acquisition of the temperature-dependent NMR data. Gas-phase data were collected at 500 MHz to maximize the separation of the ¹H TFAPYR signals and, therefore, increase the temperature interval over which rates could be extracted. It is well-known that the exchange temperature interval depends on the frequency difference, $\delta\nu$, between the sites involved in the exchange. On the other hand, ¹³C spectra of 10% (v/v) and neat TFAPYR solutions were collected at 300 MHz to lower their exchange temperature intervals and enable the inclusion of fast-exchange data in the final analysis.

The 500-MHz ¹H NMR spectrum of gaseous TFAPYR exhibits slow exchange below 294 K, coalescence at 348 K, and fast exchange above 393 K. The resulting internal rotational Gibbs free energy of activation barrier, $\Delta G^{\ddagger}_{298}$, is found to be lower in the gas phase (71.4 kJ mol⁻¹) than in any of the solutions examined. The $\Delta G^{\ddagger}_{298}$ values for TFAPYR in toluene, 1,1,2,2-tetrachloroethane, and neat (78.6, 80.9, and 80.4 kJ mol⁻¹, respectively) also exhibit solvent dependence. Toluene-d_8 and 1,1,2,2-tetrachloroethane-d_2 were chosen for their solubility properties, high boiling points (toluene bp = 111 °C; 1,1,2,2-tetrachloroethane bp = 145 °C), and dielectric constants. Toluene has a relatively small dielectric constant ($\epsilon = 2.4$) compared to 1,1,2,2-tetrachloroethane ($\epsilon = 8.2$), and neat TFAPYR is expected to have an even higher ϵ value, based on its relatively high dipole moment ($\mu = 5.33$ D; calculated using TFAPYR's ground-state geometry optimized with Gaussian 98.) Free-energy activation barriers in amides are known to increase with increasing solvent polarity, which is directly related to dielectric constant.[4,23] In this study, the dielectric constants are in the order toluene < 1,1,2,2-tetrachloroethane < neat, and the solution $\Delta G^{\ddagger}_{298}$ values are in the order toluene < neat <

TABLE 5: Gas-Phase $\Delta G^{\ddagger}_{298}$ for Selected NR$_2$-Substituted Trifluoroacetamides

		$\Delta G^{\ddagger}_{298}$ gas (kJ mol^{-1})	$\angle$C6NC5	$\angle$C6NC2	$\angle$C5NC2
***N,N*-dimethyl**		68.6 (2.1)[a]	118.09	127.15	114.76
***N,N*-diethyl**		67.4 (0.4)[b]	115.62	126.84	117.50
***N*-pyrrolidine**		71.4 (1.2)	118.33	129.18	112.33

[a] Reference 11. [b] Reference 23.

1,1,2,2-tetrachloroethane. The higher $\Delta G^{\ddagger}_{298}$ value for 1,1,2,2-tetrachloroethane is not completely unexpected because halogenated solvents are known to enhance the solvent polarity of their solutions.[24]

Only one other study has addressed the effect of cyclic substituent ring size on barriers to amide rotation. [25] In the ^{13}C NMR study of *N*-acetylpyrrolidine, Pinto et al. measured the $\Delta G^{\ddagger}$ of the internal rotation around the C—N bond to be 81.2-(0.8) kJ mol^{-1} in (CD$_3$)$_2$SO, determined at the coalescence temperature of 403.7 K. This barrier fits within the solvent dielectric series because the value of ϵ for (CD$_3$)$_2$SO (46.7) is higher than the value for toluene and lower than the expected value for neat TFAPYR (the value of μ for (CD$_3$)$_2$SO is 3.9 D, compared to 5.33 D calculated for TFAPYR).

It is also noteworthy to compare the gas-phase $\Delta G^{\ddagger}_{298}$ value of *N*-alkyl versus this *N*-cyclic trifluoroacetamide. True and LeMaster and co-workers have done extensive studies on the gas-phase barriers to rotation for trifluoroacetamides and have evaluated the results in terms of substituent bulkiness.[4,26] The current understanding is that the ground-state structures of trifluoroacetamides are destabilized by bulky *N*-substituent groups. The destabilization is attributed to steric hindrance and the concomitant loss of the amide group planarity.[23] This trend is seen not only in the trifluoroacetamides but also in the acetamides and formamides.[26] The cyclization of the alkyl side chains in pyrrolidine pulls the CH$_2$ groups away from both the carbonyl electrons and the fluorines decreasing the bulkiness around the amide nitrogen. Table 4 lists and Figure 5 illustrates some of the computational molecular parameters obtained at the MP2/6-311+G* level for the ground-state geometry of TFAPYR.

This calculation predicts ground-state planarity of the amide moiety ($\tau_{OC6NC5} = -0.90°$) and $\angle$C6NC5, $\angle$C6NC2, and $\angle$C5NC2 angle values of 118.33°, 129.18°, and 112.33°, respectively. In comparison, the same MP2/6-311+G* level ground-state calculations for dimethyl and diethyl trifluoroacetamide reveal similar planarity but smaller $\angle$C6NC5 and $\angle$C6NC2 angles. Table 5 lists the values of these angles and the corresponding gas-phase free energy of activation barriers for all three compounds.

The height of the free energy of activation barrier does not determine the relative populations of the cis and trans rotational conformers, but it definitely restricts the interconversion between them. The role of proline peptide bonds as conformational switches in proteins is based on their relatively large barrier to internal rotation and their relatively small energy difference between cis and trans conformers. We expect TFAPYR to have an internal rotation $\Delta G^{\ddagger}_{298}$ comparable to that of the standard peptide analogue *N*-methyl trifluoroacetamide. Unfortunately,

there is no gas-phase value available for the internal rotation $\Delta G^{\ddagger}_{298}$ of *N*-methyltrifluororacetamide to compare because only the strongly favored cis configuration is experimentally observed at different temperatures.[27] Nevertheless, internal rotation $\Delta G^{\ddagger}_{298}$ values for *N*-methylacetamides are known to be relatively large (a value of 87.0 kJ mol^{-1} for *N*-methylacetamide in 1,2-dichloroethane has been reported). The dielectric constant for 1,2-dichloroethane is known to be $\sim$10 comparable to 1,1,2,2-tetrachloroethane's dielectric value of 8.2. The $\Delta G^{\ddagger}_{298}$ value for TFAPYR in 1,1,2,2-tetrachloroethane is 80.9 kJ mol^{-1}. Therefore, the peptide bond in proline is expected to have an internal rotation $\Delta G^{\ddagger}_{298}$ of similar magnitude to TFAPYR and to primary amide bonds in peptides.

In the typical primary amide peptide bonds, steric conflicts between adjacent α-carbon substituents destabilize the cis configuration sufficiently that less than 1% of peptide bonds overall have a cis preference. The energy difference between the cis and trans isomers of the peptide bond analogue *N*-methylacetamide has been calculated to be $\sim$11 J mol^{-1}.[28] In comparison, the energy difference between the cis and trans configurations in proline has been found to be only 2.1 kJ mol^{-1} because of the similar steric environments for the ring α-carbon substituents in both configurations. This small difference in energy probably accounts for the higher percentage ($\sim$5%) of proline found in the cis configuration.[8] This combination of relatively high barrier to internal rotation and relatively small energy difference between cis and trans configurations seems to be ideal properties for proline to have in its role as a switch.

We conclude that the internal rotation around the C—N amide bond in *N*-trifluoroacetylpyrrolidine is much faster in the gas phase than in solution, following similar patterns found in other substituted amides. The five-membered ring substituent in TFAPYR reduces the bulkiness around the C—N amide bond, compared to *N,N*-dimethyl- and *N,N*-diethyltrifluoroacetamide, stabilizing the ground state and increasing the $\Delta G^{\ddagger}_{298}$. The magnitude of the internal rotation barrier $\Delta G^{\ddagger}_{298}$ in TFAPYR is comparable to that found in primary amide peptide bonds, emphasizing the importance of the relatively small energy difference between cis and trans conformations in proline's role as a switch in protein signaling.

References and Notes

(1) Stewart, W. E.; Siddall, T. H. I. *Chem. Rev.* **1970**, *70*, 517.

(2) Wiberg, K.; Rush, D. J. *J. Am. Chem. Soc.* **2001**, *123*, 2038.

(3) Bragg, R. A.; Clayden, J.; Morris, G. A.; Pink, J. H. *Chem.—Eur. J.* **2002**, *8*, 1279.

(4) True, N. S.; Suarez, C. *Adv. Mol. Struct. Res.* **1995**, *1*, 115.

(5) Taha, A. N.; Neugebauer-Crawford, S. M.; True, N. S. *J. Phys. Chem. A* **2000**, *104*, 7957.

(6) Hao, B.; Gong, W.; Ferguson, T. K.; James, C. M.; Krzycki, J. A.; Chan, M. K. *Science* **2002**, *296*, 1462.

(7) Marks, D. B.; Marks, A. D.; Smith C. M. *Basical Medical Biochemistry. A Clinical Approach*; Williams and Wilkins: Baltimore, MD, 1996.

(8) MacArthur, M. W.; Thornton, J. M. *J. Mol. Biol.* **1991**, *218*, 397.

(9) Brazin, K.; Mallis, R. J.; Fulton, D. B.; Andreotii, A. H. *Proc. Natl. Acad. Sci. U.S.A.* **2002**, *99*, 1899.

(10) Duffy, E. M.; Severance, D. L.; Jorgensen, W. L. *J. Am. Chem. Soc.* **1992**, *114*, 7535.

Internal Rotation in *N*-Trifluoroacetylpyrrolidine

J. Phys. Chem. A, Vol. 107, No. 17, 2003 **3029**

(11) Ross, B. D.; True, N. S.; Decker, D. L. *J. Phys. Chem.* **1983**, *87*, 89.

(12) Ross, B. D.; Wong, L. T.; True, N. S. *J. Phys. Chem.* **1985**, *89*, 836.

(13) Ammann, C.; Meier, P.; Merbach, A. E. *J. Magn. Res.* **1982**, *46*, 319.

(14) (a) Stephenson, D. S.; Binsch, G. Program No. 365. (b) LeMaster, C. B.; LeMaster, C. L.; True, N. S. *DNMR5*; Program Nos. 569 and QCMP059; QCPE, Indiana University: Bloomington, IN.

(15) Frisch, M. J.; Trucks, G. W.; Schlegel, H. B.; Scuseria, G. E.; Robb, M. A.; Cheeseman, J. R.; Zakrzewski, V. G.; Montgomery, J. A., Jr.; Stratmann, R. E.; Burant, J. C.; Dapprich, S.; Millam, J. M.; Daniels, A. D.; Kudin, K. N.; Strain, M. C.; Farkas, O.; Tomasi, J.; Barone, V.; Cossi, M.; Cammi, R.; Mennucci, B.; Pomelli, C.; Adamo, C.; Clifford, S.; Ochterski, J.; Petersson, G. A.; Ayala, P. Y.; Cui, Q.; Morokuma, K.; Malick, D. K.; Rabuck, A. D.; Raghavachari, K.; Foresman, J. B.; Cioslowski, J.; Ortiz, J. V.; Stefanov, B. B.; Liu, G.; Liashenko, A.; Piskorz, P.; Komaromi, I.; Gomperts, R.; Martin, R. L.; Fox, D. J.; Keith, T.; Al-Laham, M. A.; Peng, C. Y.; Nanayakkara, A.; Gonzalez, C.; Challacombe, M.; Gill, P. M. W.; Johnson, B. G.; Chen, W.; Wong, M. W.; Andres, J. L.; Head-Gordon, M.; Replogle, E. S.; Pople, J. A. *Gaussian 98*, revision A.6; Gaussian, Inc.: Pittsburgh, PA, 1998.

(16) Neugebauer Crawford, S. M.; Taha, A. N.; True, N. S.; LeMaster, C. B. *J. Phys. Chem. A* **1997**, *101*, 4699.

(17) Ng, S. *J. Chem. Soc. A* **1971**, 1586.

(18) Drakenberg, t.; Lehn, J. M. *J. Chem. Soc., Perkin Trans. 2* **1972**, 532.

(19) Lambert, J. B.; Oliver, W. L. J. *J. Am. Chem. Soc.* **1969**, *91*, 7774.

(20) Anet, F. A. L.; Osyany, J. M. *J. Am. Chem. Soc.* **1967**, *89*, 352. The ΔG values from this paper were recalculated and reported by Jennings, W. B.; Boyd, D. R. Strained Rings. In *Cyclic Organonitrogen Sterodynamics*; Lambert, J. B., Takeuchi, Y., Eds.; VCH Publishers: New York, 1991.

(21) Riddell, F. G. The Stereodynamics of Five-Membered Nitrogen-Containing Rings. In *Cyclic Organonitrogen Stereodynamics*; Lambert, J. B., Takeuchi, Y., Eds.; VCH Publishers Inc.: New York, 1991; p 159.

(22) Sandstrom, J. *Dynamic NMR Spectroscopy*; Academic Press: New York, 1982.

(23) Suarez, C.; LeMaster, C. B.; LeMaster, C. L.; Tafazzoli, M.; True, N. S. *J. Phys. Chem.* **1990**, *94*, 6679.

(24) Perng, B. C.; Newton, M. D.; Raineri, F. F.; Friedman, H. L. *J. Chem. Phys.* **1996**, *104*, 7153.

(25) Pinto, M. B.; Grindley, T. B.; Szarek, W. A. *Magn. Reson. Chem.* **1986**, *24*, 323.

(26) LeMaster, C. L.; LeMaster, C. B.; True, N. S. *J. Am. Chem. Soc.* **1999**, *121*, 4478.

(27) True, N. S.; Ross, B. D. *J Phys. Chem.* **1984**, *88*, 3216.

(28) Langley, C. H.; Allinger, N. L. *J. Phys. Chem. A* **2002**, *106*, 5638.